Enhancing Tunnel and Cavern Designs through Seismic Tomography and Numerical Ground Information Modelling (GIM) of Rock Mass Quality Data

Francis Lee, Alexander N. Al-Nuaimi & Michiel Van Der Laarse

AtkinsRéalis Asia Limited, Hong Kong, China

Jim Whiteley, Edward Cox & Samuel Oakley

AtkinsRéalis, GE&T

Richard Hale & Lo Leung

EGS (Asia) Ltd

doi: https://doi.org/10.21467/proceedings.7.7.4

ABSTRACT

A robust site investigation is pivotal in the design of tunnel and caverns, and collected data often defines the characterization and parameterization of rock mass quality, interpretation of geological features, and understanding of constraints of deep weathering profiles and fault zones. Conventional geotechnical site investigations (SI) for such projects typically rely on intrusive methods, such as drillholes, which provide localized samples and data. However, the isolated nature of these drillhole locations necessitates the extrapolation of geological surfaces, often leading to challenges in accurately estimating the extent, trend, and impact of geological features on adjacent rock mass quality.

To address these challenges, this study discusses how non-intrusive cross-hole seismic tomography can be used to enhance site investigations and as an input for developing integrated numerical modelling applications. This approach allows for more spatially complete evaluation of the lateral and vertical variability of rock mass quality at proposed tunnel and cavern sites. A notable aspect of this work is the exploration of correlations between seismic wave velocities and Rock Mass Quality Q-System as outlined by Grimstad and Barton (1993) and updated by Barton (2002). Additionally, the paper introduces methods for developing confidence intervals and Ground Information Models (GIM) of digital data trends.

The paper also provides a review of the benefits and limitations of these methods, along with suggestions for enhancing the geostatistical prediction of rock mass quality.

1 INTRODUCTION

1.1 Site Investigation for Tunnel and Cavern Studies

Site investigations (SI) are pivotal to characterizing ground conditions for tunnel and cavern projects and ensure designs are well-informed with a robust understanding of subsurface conditions, their constraints, engineering behavior and performability. For tunnel and cavern studies, SI targets the testing and contextualization of rock mass properties—such as strength and geological structure—to derive rock mass quality, identify and interpret geological

Proceedings DOI: 10.21467/proceedings.7.7; Series: AIJR Proceedings; ISSN: 2582-3922; ISBN: 978-81-989164-3-3

features, and predict weathering profiles and potential fault zones.

Intrusive techniques such as drillholes are used to inform classification systems such as the Rock Mass Quality Q-System (Grimstad & Barton, 1993). However, the isolated nature of conventional SI sampling often leads to challenges in accurately estimating and extrapolating trends in rock mass quality between drill holes. Moreover, isolated samples may not capture the full extent of geological features, leading to ground risk associated with limited confidence and gaps between data positions.

To reduce uncertainty, additional drillholes are often constructed to close geospatial gaps in data density. Alternatively, non-intrusive geophysical surveying techniques can be prescribed to supplement and optimize drillhole sampling (Whiteley & Cox, 2023) and close gaps between data points, producing continuous profiles. Cross-hole seismic survey is a technique that is used to measure the travel time of seismic waves between drillholes. These waves can be compressional wave (P-wave) or shear wave (S-wave), depending on the type of seismic source. The travel times and wave amplitudes are measured and variations interpreted to derive lithological boundaries, rock density and permeability.

This paper will examine the cross-hole seismic data collected between drillholes, and how it informs the design of two tunnel and cavern studies in Hong Kong, referred to as Cavern A and B. It also discusses the methodology to assess rock mass quality between project-specific drillholes. The results were also used to construct integrated numerically driven Ground Information Models (GIM), that represent data driven 3D representations of the distribution of rock mass quality across the cavern sites.

2 BACKGROUNDS OF THE STUDY

2.1 Site Description and Site Investigation Planning including Cross-hole Seismic Surveys

Cavern A and Cavern B encompass cavern sites spanning more than 20m. A site-specific Ground Information Model (GIM) was developed at the initial stage of the projects. Both locations are situated beneath densely vegetated hillsides with slope angles ranging from 25° to 45°. Geology at both sites is characterized by fine-grained and fine-to-medium-grained granite. Structural geological features such as photolineaments, identified as inferred geological features (GFs), are present at both sites and designated as GFA for Cavern A and GFB for Cavern B.

During SI planning, the geological features represented potential weak zones associated with preferential weathering of in-situ rock. Specifically, weak zones correspond to areas exhibiting continuous occurrences of 'Grade IV/V Granite' (GEO, 2017) extending below expected bedrock levels. To validate inferred trends, intrusive drillholes were strategically positioned to intercept and sample ground conditions along these inferred alignments. Rock samples recovered as 'Grade IV/V Granite' or where 'No Recovery' is recorded represent weak zones. The number of inferred geological features for Cavern A and Cavern B is two and four respectively.

The identification of potential reductions in rock mass quality linked to weak zones and faults is a fundamental aspect of both studies. Drillholes offer isolated windows of observation, however, their limited coverage and scale may lead to the omission of local weak zones and geological features. To address this, both studies conducted cross-hole seismic surveys between vertical drillholes to augment data coverage and elucidate observable trends in weak zones and seismic data related to faults, if present.

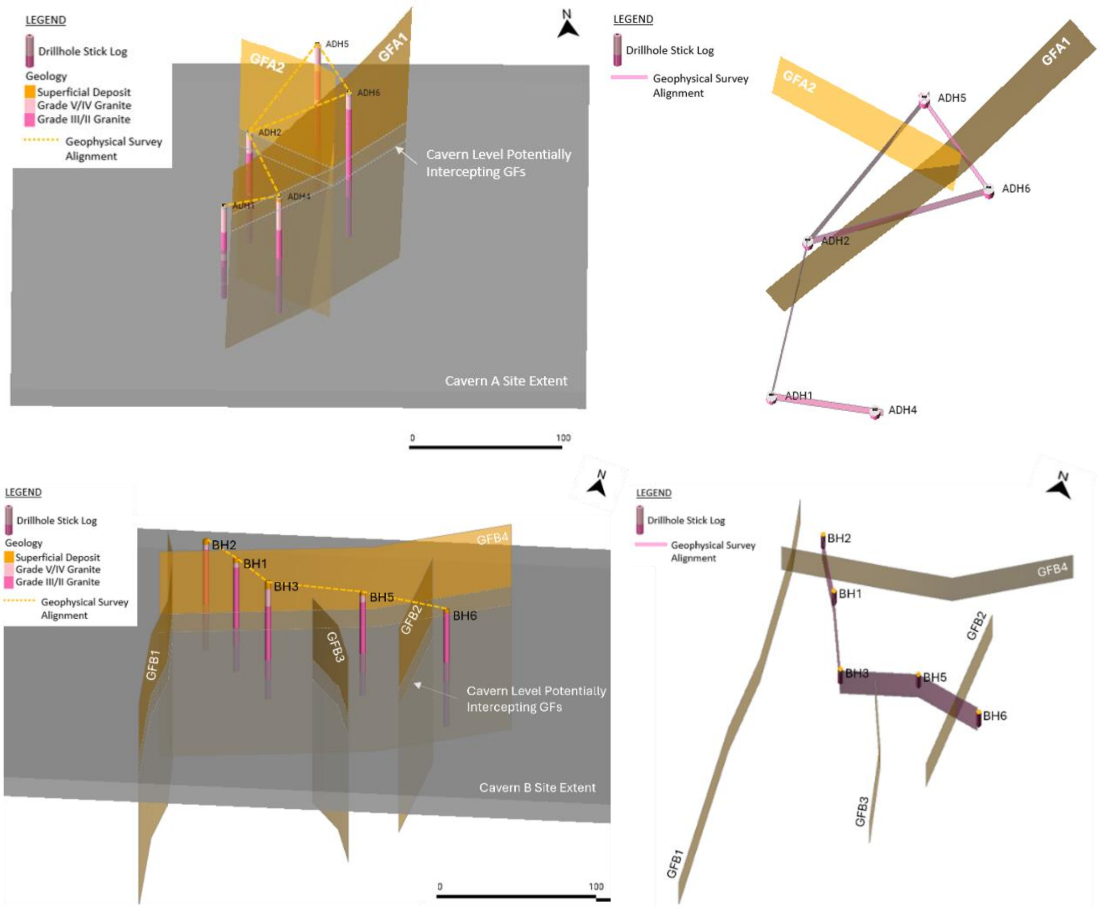

Figure 1: Configuration of Cross-hole seismic survey in relation to inferred geological features and cavern level. Cavern A (upper) and Cavern B (lower).

To ensure adequate sonification across the cavern level, drillholes were drilled to depths below the invert level. The alignment and geometry between the source and receiver drillholes were planned to intercept the potential alignments of GFA and GFB. The spacing between drillholes for the cross-hole seismic surveys was maintained at around 60m. In Cavern B, a triangular configuration was established to create a closed-loop velocity model, which facilitates visualization and interpolation in 3-dimensions (Figure 1).

3 FIELD SETUP

3.1 Site Set Up and Seismic Survey Procedures

To map geological structures between pairs of holes, very tight measurement tolerances are required, including expected accuracy of the seismic traveltime within ±0.25 ms. This ruled out the use of air guns or other low-frequency seismic sound sources. High-frequency sources, such as piezo-electric transducers working above ~10 kHz, would attenuate rapidly with distance and would not provide adequate signal-to-noise ratio over the distance between pairs of holes. A mid-frequency sparker sound source was selected to generate the most power between 1 kHz and 2 kHz.

Helicopter lifts were used to mobilize equipment to the drillhole location. For each pair of holes, the set up included a multi-channel hydrophone string (with 1 m element spacing) lowered down a receiver drillhole and a sparker sound source lowered down the other. Figure 2 (left) shows the seismograph display used on site to check

Proceedings DOI: 10.21467/proceedings.7.7
ISBN: 978-81-989164-3-3

Series: AIJR Proceedings
ISSN: 2582-3922

the quality of the seismic records. The sparker sound source was raised to the next level and another set of seismic traveltimes was recorded. This was iterated all the way up to rockhead, until a dense network of seismic rays covered the region between the pair of holes. Figure 2 (right) is a composite seismic record, with sound source at +81 m PD (marked by a red "X"). The hydrophone receivers are from the base of opposite drillhole (+52 m PD) up to just above rockhead (+137 m PD). The seismic traveltime is taken as the onset of the seismic arrival, indicated by a rise above background noise levels. Automatic traveltime picks were made, supplemented by the judgement of the geophysicist on site. The automated process for identifying the first break-peaking was informed by a theoretical range of tolerance. Within each data trace, energy or amplitude changes were detected by applying a gradient threshold. Once the setup was ready, following a strong shot instant pulse record and the seismic traveltimes can be observed clearly.

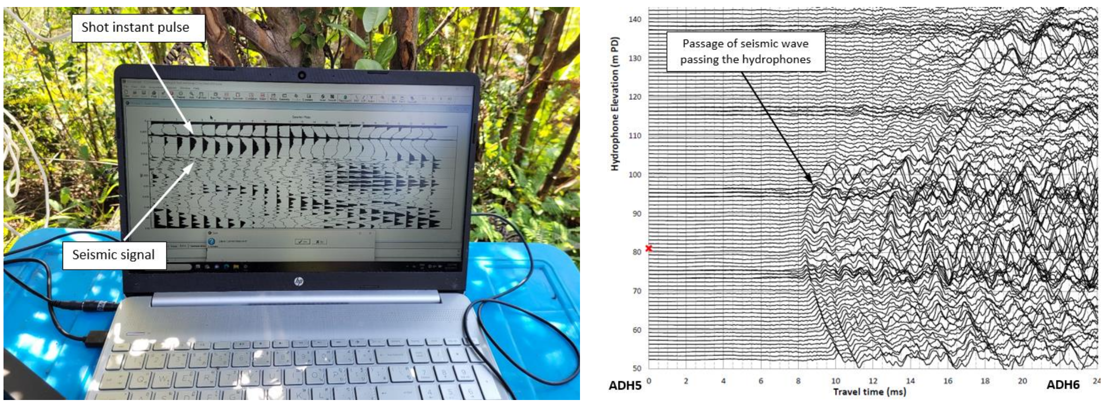

Figure 2: Type of display used by the geophysicist to check the quality of seismic records (left). Example of seismic record, seismic pair from drillholes ADH5 to ADH6 (middle).

4 DATA PROCESSING

4.1 Seismic Processing and Measuring Traveltimes

By design, around 5% of shot-receiver pairs were duplicated to accomplish statistically independent duplicate measurement. The measurements will seldom be identical, but the distribution of the difference in measurements is a robust estimate of the measurement accuracy. During the works of both Cavern A and Cavern B, there were 1447 repeat measurements, in which 96% of the repeat measurements (roughly two standard deviations) were within ±0.10 ms. This was comfortably inside the planned tolerance of ±0.25 ms, validating the survey design.

4.2 Tomographic Inversion

Variations in traveltime can be divided into two components: geometrical effects (the greater the separation between the source and receiver, the greater the traveltime) and the variation of seismic velocities. The algorithm separating these factors to produce an image of seismic velocities is computed in EGS-proprietary in-house Tomographic Inversion software.

The section between source and receiver holes was divided into 5m-by-5m cells. The resulting 5m grid resolution was selected considering the geometry, the distance between the holes and the number of traveltimes measured. A limitation associated with the 5m resolution of seismic survey is that smaller geological features will be 'averaged' over the resolution scale. In future studies, forward-modelling can help to inform the resolution of a given array design, and therefore the size of minimum detectable features. Such forward models can either be from of the assumed ground conditions (informed by pre-existing geological data and desk studies) (Rücker et al., 2017) or using synthetic examples such as checkerboard tests combined with considerations of ray-path coverage (Rawlinson and Spakman, 2016). The outputs of these studies can be used to optimize the cross-hole array design.

For each seismic source, wave fronts were projected through the model of the rock to the receiver positions. A finite difference algorithm was used according to Rawlinson and Sambridge (2005) with bending according to Snell's law of refraction.

For the initial constant-velocity model, the average misfit between measured and calculated traveltimes was ±0.8 ms. This average misfit was considerably greater than the measurement accuracy, ±0.1 ms, indicated by the results of repeated measurements discussed in Section 4.1.

The modelling process adjusts the seismic velocities of each grid cell, with the objective of making the average misfit less than the measurement accuracy. A grid cell was selected at random and its velocity incremented up or down – a trial value. All traveltimes were recalculated in each iteration. If the overall traveltimes were closer to the measured values (reduced discrepancy), the trial value was accepted. Even if the traveltimes were worse using the trial value (increased discrepancy), there was still a finite chance that the change would be accepted. During the initial "fluidisation" phase, all trials were accepted, which increased the misfit to around ±1.0 ms. Over hundreds of thousands of iterations, the chance of accepting a worse value was gradually lowered, a process known as the Monte Carlo annealing schedule. As the number of trials goes on, the selection of seismic velocities becomes less random and converges on the velocities that have given the best calculated traveltimes.

For all iterations for these pairs of holes, after considering 200,000 trial seismic velocities, the final average discrepancy was close to or less than the measurement accuracy of ±0.10 ms. Each iteration finished with a similar, but not identical, final model of seismic velocities. The average of these iterations provides the best unbiased estimate of seismic velocities. The variation between iterations is a fundamental estimate of the accuracy of the results. Examples of inversed velocity models are presented in Figure 3. These models can be visualized using software packages like Oasis Montaj, or in voxel model.

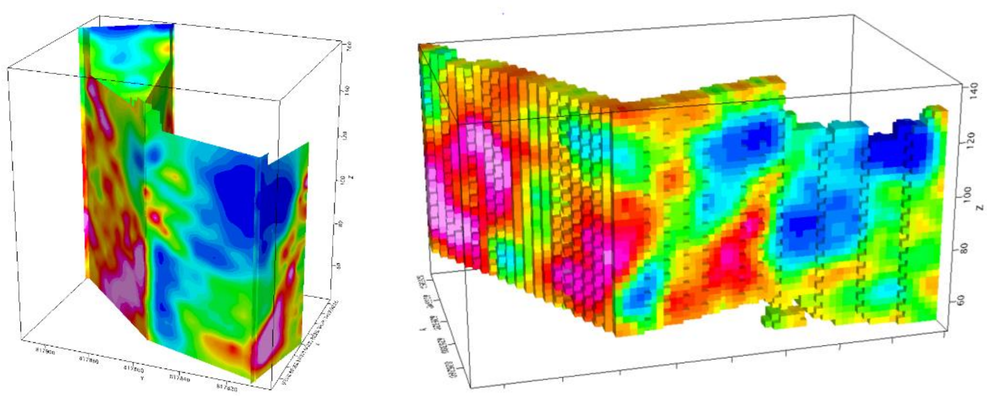

Figure 3: 3D seismic velocity model imported into Oasis Montaj for Cavern A (left) and seismic velocity data voxel model for Cavern B (right).

4.3 Developing Confidence Limits for Results

Presenting the results is of little use to the Engineer without also presenting a quantified assessment of the accuracy and reliability. The following sections describe how the confidence limits were represented and visualized using statistical measurement (standard deviation) and density coverage (raypath coverage model).

4.3.1 Standard Deviation

The uncertainty of seismic velocities is calculated using the statistical measure of standard deviation. The accuracy was calculated by iteration of the tomographic inversion described in Section 4.2, each time using a different random number sequence in the Monte Carlo process. Each iteration has a different random combination of trials, so each will converge on a slightly different result. Although the resulting distribution of seismic velocities is slightly different from one pass to another, all passes gave a similar accuracy in representing the measured seismic traveltimes. The standard deviation of the distribution of the differences between one pass and another equals the standard deviation of the seismic velocities. Figure 4 shows histograms of standard deviations calculated in all cells in the final models for Cavern A (left) and Cavern B (right) projects respectively. In Cavern A, with relatively heterogeneous conditions, around 90% of values were within ±0.6 m/ms. In Cavern B, with more uniform geology, around 90% of values were within ±0.3 m/ms.

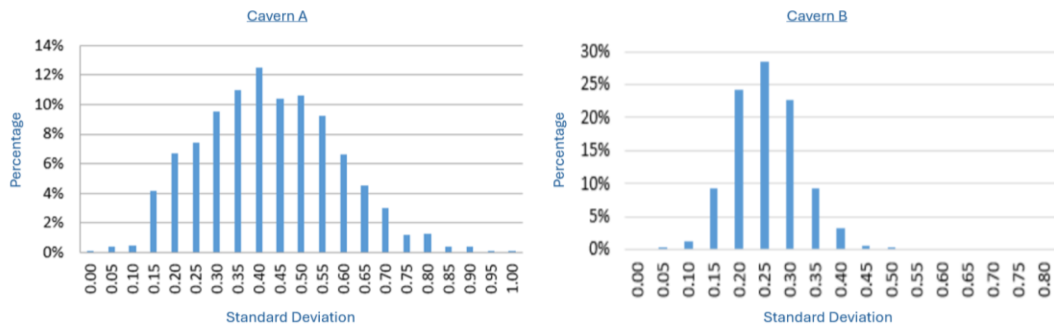

Figure 4: Histograms of standard deviations in seismic velocity. Cavern A (left) and B (right).

4.3.2 Raypath Coverage

While standard deviation describes how well the inversion model fits the data, it does not illustrate the extent of seismic data coverage. At locations where a spatial inversion window model has few or no measured data points available, the inversion process will still generate seismic velocity values and may still output a low standard deviation for the generated seismic velocity values. Therefore, a second phase of processing was undertaken to ascertain a better spatial indication of potential seismic velocity data.

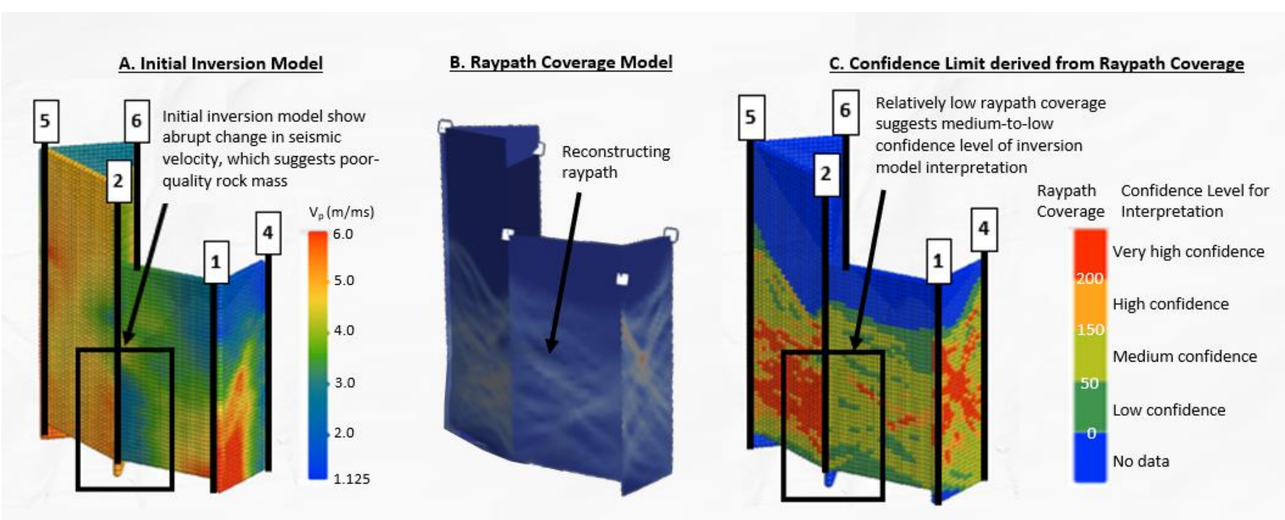

Figure 5: Process of developing confidence limit of seismic inversion model through analysing its raypath coverage.

Additional inversions were run using pyGIMLi (Rücker et al., 2017), which act as independent verification of the Monte Carlo inversion results described in Section 4.2. The ray-path coverage from the pyGIMLi inversion was used to apply confidence limits to the results of the tomographic inversion. The additional inversions also produced models showing the seismic raypath coverage (Figure 5). *Coverage* is the sum of ray lengths having crossed each cell of each model. In Cavern A, the maximum value for coverage was 506 with a lower quartile of 76.64 and an upper quartile of 217.96. Confidence intervals were suggested based on this statistical analysis. Comparison of the initial tomographic inversion described in Section 4.2 and the additional inversions using pyGIMLi showed good agreement in terms of seismic velocity distribution.

The spatial distribution of coverage can be used to qualitatively assess co-located seismic velocity data, areas with low data coverage having a lower confidence of result certainty. For example, an area showing an unusually abrupt change in seismic velocity (Figure 5a) was observed in borehole ADH2 of Cavern A, which possessed relatively lower raypath coverage (Figure 5b), suggesting the seismic velocity inversion should be treated with low-to-medium confidence at this area (Figure 5c). During data integration, data recorded in low confidence zones were generally excluded from ground modelling.

5 INFORMING ROCK MASS QUALITY BY SEISMIC TOMOGRAPHY RESULTS

5.1 Quantitative Seismic Data for Numerical Modelling

Apart from Ground Information Model (GIM) acknowledging the site-specific ground condition, numerically informed, quantitative GIM were also developed to provide data-driven 3D representations of the distribution of rock mass quality Q-value using Leapfrog Works Version 2023.2 (Seequent, 2023). The spheroidal variogram model (interpolant function) was used to model predicted lateral and vertical variability of Q-value distribution at Cavern A and B. The spherical interpolation function has a fixed range beyond which the value transitions into a constant sill. This provided a means for rationalizing the influence of variable data density, in this case, differences in influence of drillholes and geophysical data. Project-specific seismic data was incorporated in GIM as 2D sections and 3D point data source for numerical modelling.

5.2 Rock Mass Quality

Assessment of Q-value along existing and project-specific rock samples was carried out adopting the Norwegian Geotechnical Institute's (NGI) Rock Mass Quality Q-system (Grimstad & Barton, 1993). This assessment considered measurements such as Rock Quality Designation (RQD), condition and number of joints and stress reduction factors associated with rock overburden.

Considering the case study at Cavern A, the sampled bedrock from drillholes is predominantly moderately to slightly weathered granite, with most of the mapped Q-value falling within a range of 0.6 to 15. At locations where weak zones (highly to completely decomposed rock mass) were recorded, mapped Q-value drops to 0.6 (very poor) and occasionally below 0.1 (extremely poor).

Interpretation of the geophysical survey data referred to Reynolds (1997), which suggests that moderately to slightly weathered granite typically corresponds to a seismic velocity range of 4.6m/ms to 6.2m/ms. Project-specific seismic measurements at Cavern A range between 2.5m/ms and 6.5m/ms. This variability indicates patterns/ variation in the occurrence of bedrock weathering grades across the site. An empirical relationship developed by Barton (2002) was employed to correlate seismic velocity with rock mass quality Q-values (Figure 6).

Proceedings DOI: 10.21467/proceedings.7.7
ISBN: 978-81-989164-3-3

ISSN: 2582-3922

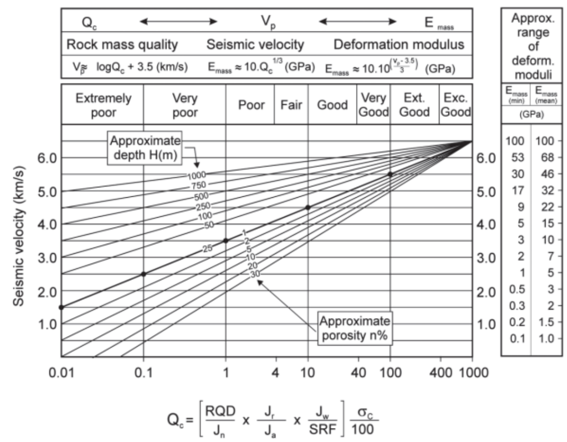

Figure 6: Velocity-depth correlation developed from case records (from Barton, 2002).

This empirical relationship considers the effect of depth, i.e. in-situ stress on rock mass with increasing depth. The presence of overburden and associated stress tends to increase V_p (P-wave velocity) for any given Q-value. Q_c is adopted as the improved correlation to Q-value where θ_c is the uniaxial compressive strength of intact rock mass (MPa) shown in eq.1. It should be noted that laboratory testing such as Uniaxial Compressive Strength (UCS) tests have been performed as part of the site investigation, indicating that a UCS value of θ_c = 70 to 195 MPa is representative of the site-specific rock mass strength for grade III to II granite.

$$Q_c = Q \times \frac{\theta_c}{100} \quad \text{(eq.1)}$$

Raypath models illustrating data coverage across Cavern A drillholes were reconstructed based on the methodology discussed in Section 4.3.2 (Figure 7a). The raypath coverage depicted in Figure 7b provided essential information regarding seismic data coverage, which was considered as part of the confidence limit assessment of the V_p and rock mass quality Q data models. Areas with a higher percentage of data coverage were interpreted with greater confidence; in this case, a confidence limit was established at not less than 150 of raypath coverage (Figure 7c). The Vp values could then be extracted from regions of high confidence for further interpretation and calculation of rock mass quality Q-values (Figure 7d).

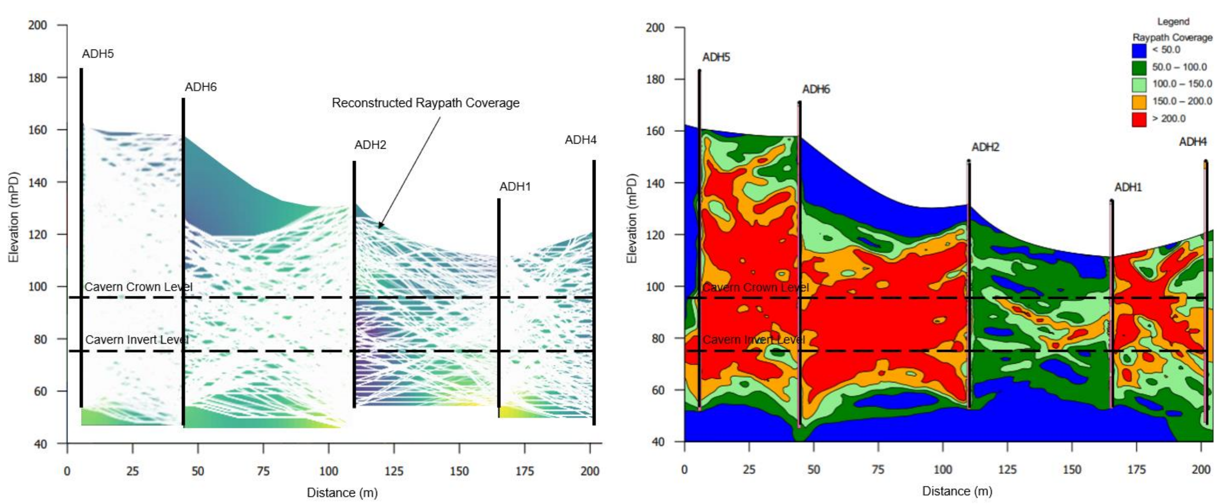

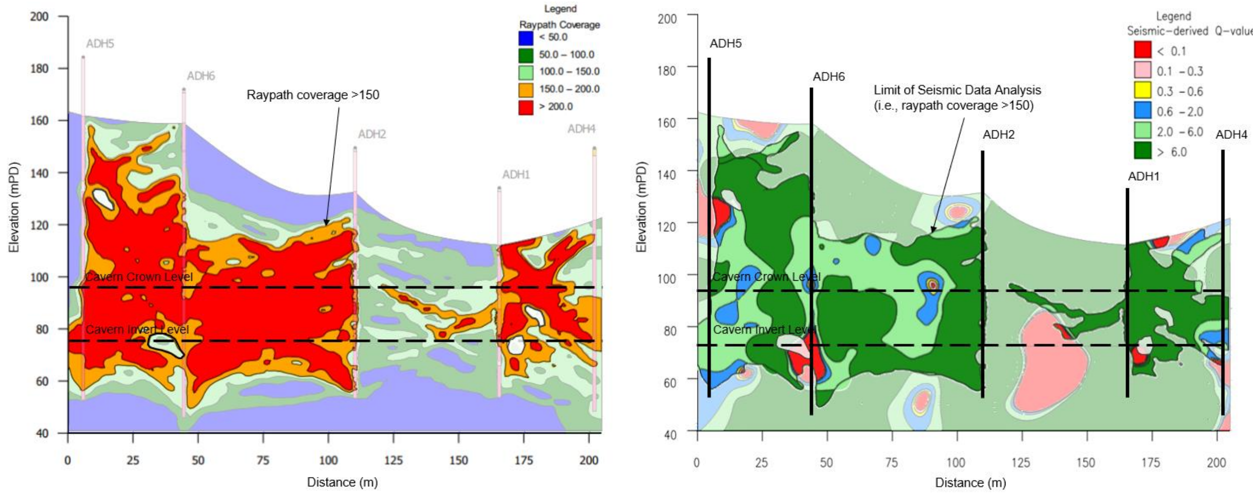

Figure 7: (a) Raypath coverage; (b) Raypath percentage coverage; (c) Raypath coverage higher than 150 is delineated and (d) Limit of seismic data analysis is delineated.

5.3 Geological Features

A key aspect of the studies conducted in Caverns A and B is the verification of the existence, extent and orientation of geological features, as discussed in Section 2. To address the possibility of drillhole locations that could miss these features, cross-hole surveys were utilized to identify seismic velocity patterns indicative of weak zones.

At the Cavern A site, a subvertical geological feature identified as GFA1 was recognized during preliminary studies. The alignment of seismic surveys ADH5-ADH6, ADH6-ADH2 and ADH1-ADH2 intersected GFA1 at three distinct locations (as shown in Figure 1) and the seismic-derived Q-value model are unfolded in Figure 8.

Along the profiles ADH5-ADH6 and ADH6-ADH2 (Figure 8), variations in seismic velocity at cavern level were evident as subvertical pockets of reduced Q-value (0.6-2.0, blue) extending from +100 to +80mPD within a predominantly higher Q-value context of >2.0 (shown in light green to dark green). These subvertical zones signified relatively sharp and confined changes in rock mass quality, correlating with the conceptual alignment of GFA1. Continuous profiling provided information on the apparent depth, immediate thickness (notably confined, as evidenced by sharp contrasts with neighboring rock masses) and the impact of GFA1 on the surrounding rock mass.

Conversely, along the ADH2-ADH1 profile (Figure 8), limited raypath coverage inhibited visualization of the rock mass quality corresponding to GFA1 at this location. Evaluation of GFA1 here necessitated reliance on supplementary site investigation data. This included considering the character of the seismic signals (such as signal-to-noise ratio, attenuation of high seismic frequencies) recorded between holes ADH2-ADH1.

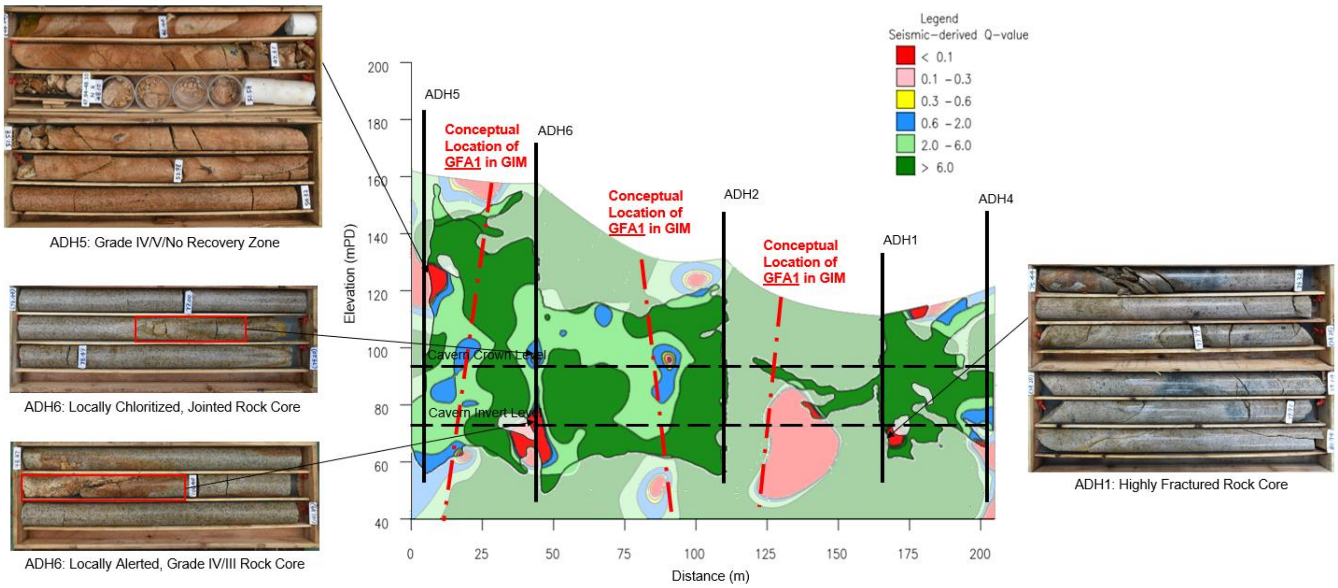

Figure 8: Comparison between seismic survey data, conceptual location of GFA1 and rock core quality along boreholes. Low seismic-derived Q-values generally consistent with rock core recovery of i) grade IV/V/ No recovery zone; ii) locally chloritized/ altered rock and iii) highly fractured rock.

At the Cavern B site, up to four geological features were recognized during preliminary studies. The alignment of seismic surveys BH2-BH1, BH1-BH3, BH3-BH5 and BH5-BH6 was positioned to intersect the geological features GFB2, GFB3 and GFB4 (as shown in Figure 1). The resulting seismic velocities are profiled in Figure 9.

Along the profiles of BH3-BH5 and BH5-BH6, two significant trends of low velocity (purple to blue) were evident, dipping at an angle of 50° and extending from +125 to +70mPD through the cavern level (Figure 9). The velocity data trends indicated a persistent change of rock mass quality in contrast with the medium to high velocities (green to red) of the neighboring rock mass, coinciding with the conceptual alignments of GFB2 and GFB3. The seismic profiles verified the apparent extent and orientation of GFB2 and GFB3 and provided information on the apparent depth and thickness of the geological features, as well as zone of influence with regard to cavern level.

The seismic result along the BH2-BH1 profile did not indicate trends of low velocity along the conceptual alignment of GFB4. Instead, mostly very high velocities (red) indicating good rock mass quality was recorded at this location. This apparently refuted the existence of GFB4, suggesting better than expected ground conditions.

Additionally, a minor subvertical trend of low velocity was evident along the profile of BH1-BH3, extending from +110 to +70mPD, suggesting the occurrence of a new feature GF? (Figure 9). The identification of GF? allowed the design to accommodate the presence of lower rock mass quality, thereby reducing ground risk and potentially avoiding additional costs at a later stage of the project.

The seismic data visualized trends in 2D tomography cross section and verified the occurrence of geological features, offering a different perspective to conventional SI. The Cavern A study highlights how continuous profiling is useful in validating initial stage results; while Cavern B study highlights how continuous profiling is useful in identifying previously unknown risks.

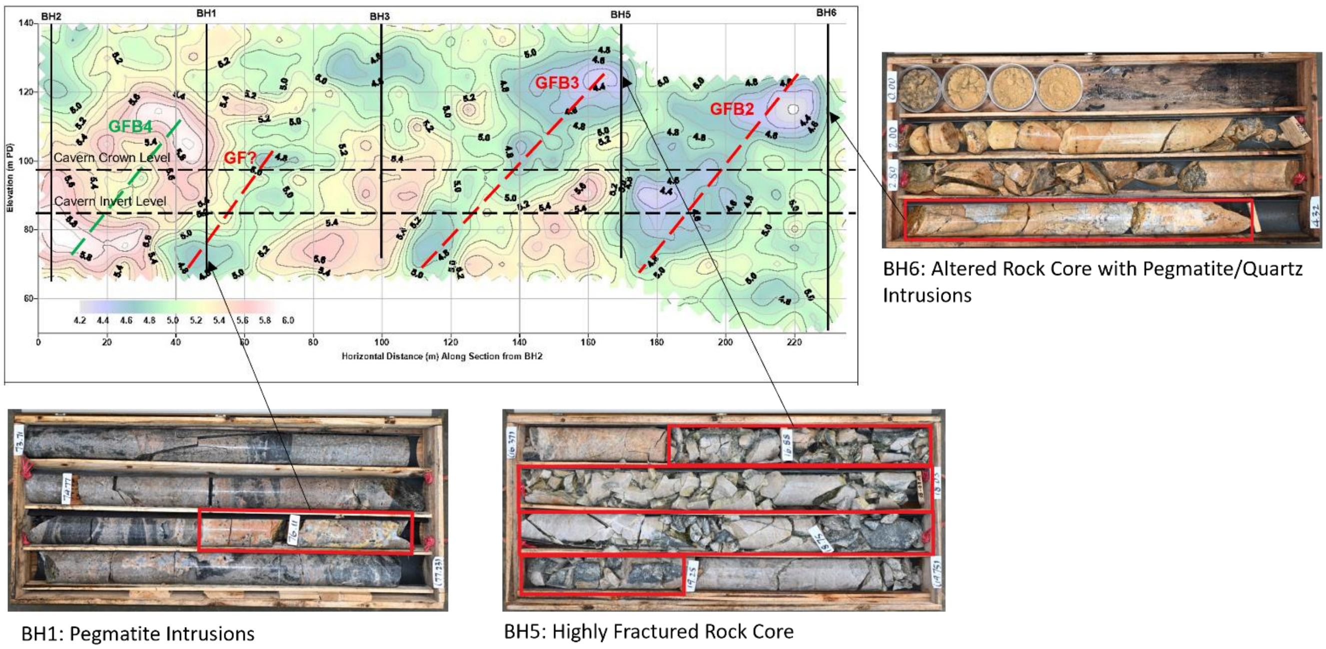

Figure 9: Seismic velocity profiled across BH2-BH1, BH1-BH3, BH3-BH5, and BH5-BH6. Red lines indicate the apparent extent and orientation of GFB2 and GFB3 based on velocity contrast, and newly identified geological feature GF?.

5.4 Informing Geotechnical Designs and Reduce Risk

Processed seismic data provides continuous 2D visualization of subsurface rock mass quality with broad coverage efficiently. This data not only provides insights into the thickness, trend, depth, and consistency of potential geological features but also facilitates informed design decisions regarding 1) cavern/tunnel layout and 2) rock mass support systems.

5.4.1 Informing Cavern/Tunnel Layout

Geological features (GFs) exhibiting varying states of weathering often present complex deformation patterns and variations in rock properties, raising concerns about stability and local stress concentration. Furthermore, these GFs may serve as conduits for groundwater flow, potentially resulting in localized high groundwater inflows during excavation activities. By understanding the orientation, depth and consistency of GFs, the layout and alignment of Cavern A and Cavern B have been optimized. This optimization includes strategies to either avoid intersections with GFs; align parallel to pre-existing weakness planes to exploit these zones of lower strength; or orient perpendicular to minimize interactions with GFs. Additionally, the location and extent of pre-excavation grouting (PEG) were planned to mitigate groundwater inflow into the underground excavations.

5.4.2 Rock Mass Quality

Rock mass quality is one of the major inputs for cavern/tunnel rock mass support system e.g. rock bolt specifications. In contrast to the isolated results obtained from conventional drillhole sampling, seismic data offers continuous measurements that reveal trends in rock mass quality, effectively filling the data gaps between drillhole points. As discussed in Section 5.1, a numerical GIM was constructed using integrated Q-values derived from seismic correlation measurements, as illustrated in Figure 10. The Q-value intervals from rock core samples varied from small (<0.5m in length) to large (>3m in length), together with the seismic derived Q-value (at a 5m grid size) were integrated in the GIM. This integration provides a more comprehensive assessment of both lateral and vertical variability in rock mass quality, thereby informing the design of rock support systems.

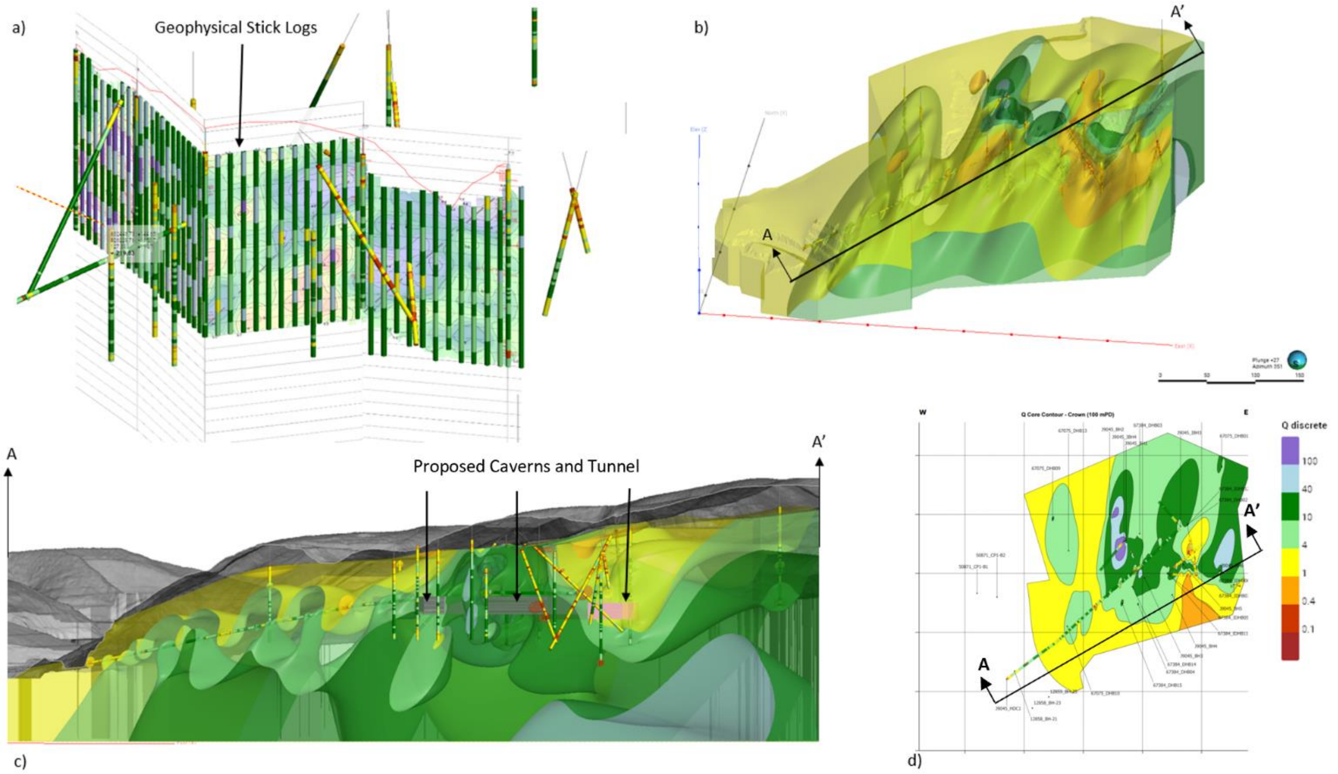

Figure 10: 3D Visualizations of a) Seismic Velocity Derived Q-Value Stick Logs, b) Predictive Q-Value Contour Visualization, c) Profile of Q-Contour along HDC1 and d) Plan View of Q-value.

6 CONCLUSION AND WAY FORWARD

6.1 Conclusion

The studies conducted at Cavern A and B demonstrate how geophysical data can be collected, processed, and utilized to evaluate the characterization and distribution of rock mass quality for tunnel and cavern sites. Although natural terrain hillsides in Hong Kong presents considerable challenges and restrictions in collecting Site Investigation (SI) data, the integration of geophysical surveys significantly enhances the value of these investigations. The resulting continuous, non-intrusive data coverage creates opportunities for apparent ground truth observations, which can be leveraged to inform interpretations of geological structures and weathering patterns, thereby assessing the ground risk associated with geotechnical designs.

This study also emphasizes the importance of implementing quality assurance checks to evaluate the consistency and accuracy of seismic measurements, enabling the isolation of high-confidence data that can be utilized in ground modeling applications. It is essential to quantify the resolution and uncertainties related to the measurements, analyses, and calculated seismic velocities, as these factors must be considered when interpreting the results.

Data-driven ground models were used to assess confidence of collected data, enhance interpretations, and mitigate ground risk along with engineering constraints. The approaches applied in this study demonstrate how geotechnical designs for tunnel and cavern studies can be supported, integrated, and enhanced by incorporating geophysical-informed site investigation efforts.

6.2 Future Opportunities

Conventional methods of interpreting Q-value in tunnel and cavern studies rely heavily on drillhole records, including their spatial positioning, density, and constructability. The ground risk associated with the alignment of infrastructure within a site changes as new geotechnical data becomes available. Increasing the density and spatial distribution of factual data collected during SI using non-intrusive techniques can reduce uncertainty and provide opportunities for time-cost savings associated with design.

The findings in this study show that geophysical surveying techniques combined with numerical modeling applications can expand data coverage and enhance the understanding of subsurface conditions, thereby informing geotechnical designs. Future studies should explore integrating enhanced stochastic/geostatistical methods to facilitate informed decision-making during the planning and construction phases.

REFERENCES

Barton, N. (2002). Some New Q-Value Correlations to Assist in Site Characterisation and Tunnel Design. International Journal of Rock Mechanics and Mining Sciences, 39 185-216.

Grimstad, E. & Barton, N. (1993). Updating of the Q-system for NMT. Proceedings of the International Symposium on Sprayed Concrete – Modern Use of Wet Mix Sprayed Concrete for Underground Support. Norwegian Concrete Association, Fagernes, Oslo.

GEO (2017). Guide to Rock and Soil Descriptions (Geoguide 3) (2017 version). Geotechnical Engineering Office, Civil Engineering and Development Department, HKSAR Government.

Rawlinson, N., & Sambridge, M. (2005). The Fast Marching Method: An Effective Tool for Tomographic Imaging and Tracking Multiple Phases in Complex Layered Media. Exploration Geophysics, 36, 341 - 350.

Rawlinson, N., & Spakman, W. (2016). On the use of sensitivity tests in seismic tomography. Geophysical Journal International, 205(2), 1221-1243.

Rücker, C., Günther, T., & Wagner, F.M. (2017). pyGIMLi: An open-source library for modelling and inversion in geophysics. Comput. Geosci., 109, 106-123.

Whiteley, J. & Cox, E. (2023). Enhancing Site Investigation for Karst Geohazards Using High-Resolution, Quasi-3D Electrical Resistivity Tomography Surveying. NSG2023 29th European Meeting of Environmental and Engineering Geophysics, Vol. 2023, No. 1, pp. 1-5. European Association of Geoscientists & Engineers.